I&EC research
Industrial & Engineering Chemistry Research

ARTICLE

pubs.acs.org/IECR

Controllable Preparation of Poly(butyl acrylate) by Suspension Polymerization in a Coaxial Capillary Microreactor

Zhendong Liu, Yangcheng Lu,* Bodong Yang, and Guangsheng Luo

State Key Laboratory of Chemical Engineering, Department of Chemical Engineering, Tsinghua University, Beijing 100084, China

ABSTRACT: In this work, a new controllable and continuous free radical polymerization process was developed and characterized in a coaxial capillary microreactor. In this process, the monomer solution was first dispersed into monodispersed droplets followed by thermal-initiated polymerization in the following capillary immersed in an oil bath. Poly(butyl acrylate) prepared in this microreactor possessed a much higher average molecular weight (M_n) and far lower polydispersity index (PDI) than that produced in a typical stirred vessel. The microreactor method possesses two unique advantages which allow for the optimization of the free radical polymerization process. First, the use of highly monodispersed droplets as polymerization units ensures that the polymerization process occurs uniformly in each individual droplet. Second, the small droplet size, on the order of several hundred micrometers, greatly enhances heat transfer efficiency with no heat accumulation within the droplets during polymerization. A simplified numerical simulation was used to show the superiority of the microreactor in effectively removing polymerization heat due to the miniaturization of the droplets to submillimeter scale. Simulation results also demonstrated that, in contrast to polymerization processes occurring in macroreactors, the polymerization conducted in the microreactor proceeded in a nearly isothermal condition. Experimental results in the microreactor showed that the molecular weight distribution was mainly determined by the size of the droplet, while the molecular weight of the polymer could be adjusted by changing the reaction temperature and 2,2-azobis(isobutyronitrile) concentration. This type of microreactor can potentially be applied to research involving the mechanisms of highly exothermic free radical polymerization processes and can also be used as an efficient tool for their controllable preparation.

1. INTRODUCTION

Free radical polymerization is one of the most widely adopted commercial processes for the preparation of high molecular weight polymeric materials.[1] The advantages of free radical polymerization are obvious: it can be applied to almost all vinyl monomers under mild reaction conditions over a wide temperature range, it is water tolerant, and its cost is relatively low. However, it also possesses several conspicuous disadvantages such as the release of a large amount of associated heat, severe variation in viscosity, and diffusion controlled termination mechanism.[2] Polymerizations are generally conducted in conventional chemical reactors such as stirred-tank reactors. However, due to inherent shortcomings such as poor mixing and low heat and mass transfer efficiencies, conventional reactors offer only a limited ability to control the polymerization process, resulting in polymers with varying degrees of conversion and polydispersity indices (PDIs).[3]

In recent years, microreactor technology has been thoroughly studied and applied to various chemical reaction processes.[4,5] Reducing the characteristic size of the reactor to the micrometer or submicrometer scale brings about a series of advantages such as a uniform flowing state, high heat and mass transfer efficiencies, and fast mixing within milliseconds.[6−8] Microreactors have already successfully been used in many different fields including organic synthesis,[9] crystallization, and precipitation.[10,11] Microreactors have also been applied to various polymerization processes including radical polymerization,[12] ionic polymerization,[13,14] photopolymerization,[15] and copolymerization.[16] Thus we can take advantage of the unique characteristics of the microreactor to potentially overcome the aforementioned drawbacks of free radical polymerization.

In their pioneering work, Iwasaki et al.[17] successfully demonstrated the advantages of using a microreactor to carry out the free radical polymerization of several monomers. Their results showed that, for a highly exothermic polymerization process such as the polymerization of butyl acrylate, significant improvement of PDI could be achieved in a microreactor compared to those obtained in batch processes. The microreactor was quite effective in controlling the molecular weight distribution for highly exothermic free radical polymerizations.

In general, microreactors have proven to be very effective and versatile when applied to processes involving free radical polymerization reactions. For example, by using a multistage microfluidic device, Li et al.[18] successfully conducted the free radical polymerization of an acrylate and polycondensation of an urethane oligomer sequentially in one device, using exothermic free radical polymerization to trigger the polycondensation. Through this internal trigger approach, the continuous preparation of polymer particles with an interpenetrating polymer network (IPN) and narrow particle size distribution could be realized. Moreover, to achieve precise control of the polymer particle properties, Okubo et al.[19] polymerized styrene and methyl methacrylate within microemulsion droplets using a K-M mixer and within segmented flow using a union tee microreactor. They demonstrated that internal circulation within the slugs contributed to removal of heat generated in the polymerization process and hence facilitated better control of polymer properties such as size and molecular

Received: May 7, 2011
Accepted: September 12, 2011
Revised: September 12, 2011
Published: September 12, 2011

dx.doi.org/10.1021/ie201497b | *Ind. Eng. Chem. Res.* 2011, 50, 11853–11862

weight distribution. However, since the slugs were in close contact with the channel wall, flowing resistance increases significantly as the polymerization proceeds, potentially resulting in clogging problems. Besides, taking advantage of the precise control over reaction time and heat transfer efficiency offered by a microreactor, Lorber et al.[20,21] proposed a microfluidic-based approach to monitor the kinetics of free radical polymerization.

In the past two decades, micro devices with various geometries including shear flowing, cross flowing, hydrodynamic focusing, and coflowing have been developed for laboratory or industrial use.[22] A coaxial micro device, as one kind of coflowing micro devices, has shown good convenience and reliability in controlling flow patterns such as drop flow, slug flow, and colaminar flow.[23,24] It has been successfully used to synthesize materials with some specific configurations, including spherical[25,26] or rodlike microparticles,[27] Janus particles,[28] ternary particles,[29] microcapsules,[30] and microtubes.[31]

The microfluidic technique is regarded to be quite different from the conventional technique in emulsion preparation.[32] Due to the miniaturized size, the interfacial tension force and viscous shear forces become dominant in the microfluidic device, instead of the inertial force in conventional devices such as stirring vessels,[33,34] which makes the droplets produced in the microfluidic device well controllable in size and flow. As reported, the size of droplets generated by a coaxial micro device is highly uniform and the CV (coefficient of variation) value could be less than 2%.[35] In addition, due to the high degree of control afforded by microfluidics, monodispersed double emulsions[36] and multiple emulsions[37] could easily be formed in microcapillary devices.

In the present work, we employed a coaxial capillary microreactor to realize a controllable suspension polymerization within monodispersed drop flow. Using this method, several characteristics of the process may potentially be enhanced. First, reaction heat removal can be enhanced by decreasing the heat transfer distance—the key to controlling a highly exothermic reaction. Second, drop flow in the capillary can provide an identical reaction time in each droplet. Finally, because the droplets are effectively separated by an immiscible, continuous inert fluid, the products or intermediates within the droplets have only a small chance of adhering to the reactor, thereby causing clogging. Thus, it may be feasible to prepare polymers with a molecular weight as uniform as possible in a continuous manner.

As mentioned above, though several works on free radical polymerization in microreactors have been reported, their focus stressed either controlling polymer particle size or studying polymerization kinetics. Currently, the characteristics of free radical polymerization in uniform flowing droplets have not been specifically investigated. The effect of droplet size on suspension polymerization is still not clear. Here we selected butyl acrylate as a typical monomer, and a controllable and continuous suspension polymerization process for the preparation of poly(butyl acrylate) was realized by using a coaxial capillary microreactor to generate monodispersed droplets with adjustable size. The reaction conversion and product properties produced using this microreactor method were compared with those of a typical stirred tank vessel representative of batch-type reactors. The influence of the phase ratio, 2,2-azobis(isobutyronitrile) concentration, and reaction time in the microreactor were also investigated to examine the key characteristics of free radical polymerization control.

Computational fluid dynamics (CFD)—capable of providing detailed views regarding localized flow patterns, mixing mechanisms, and concentration and temperature profiles—can be used effectively for studying a number of polymerization processes such as bulk polymerization,[38] suspension polymerization,[39] and emulsion polymerization.[40] In this work, in order to provide deeper insight into the superiority of the microreactor in coping with highly exothermic free radical polymerization reactions, a simplified CFD simulation was carried out to calculate the temperature profile within individual butyl acrylate droplets during the polymerization process. CFD simulation results were expected to provide an instantaneous relationship between heat release and heat removal, and the influence of droplet size on that relationship.

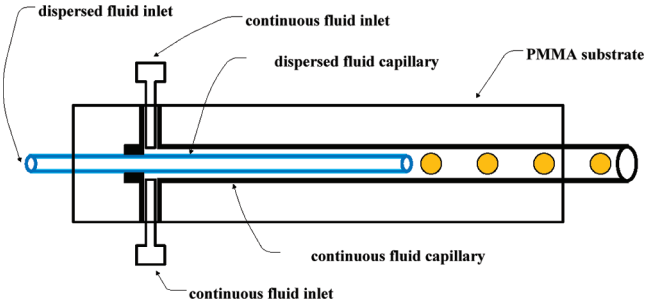

Figure 1. Scheme of coaxial capillary microreactor.

2. EXPERIMENTAL SECTION

2.1. Materials. Butyl acrylate (BA), 2,2-azobis(isobutyronitrile) (AIBN), sodium dodecyl sulfate (SDS), poly(vinyl alcohol) (PVA), sodium hydroxide (NaOH), and sodium sulfate (Na_2SO_4) were of analytical grade. BA and AIBN were obtained from Sinopharm Chemical Reagent Co. (Beijing, China) and TongGuang Fine Chemicals Company (Beijing, China), respectively. The other chemicals were from Beijing Chemical Works (China). To remove inhibitor, BA was washed with 1 M NaOH three times, washed with water three times, and dried with Na_2SO_4. Before use, BA monomer and water were stripped with N_2 to remove dissolved O_2 for at least 1 h. Other materials were used as obtained.

2.2. Experiments. *Fabrication of Coaxial Capillary Microreactor.* Figure 1 shows the layout of the coaxial capillary microreactor. The device was fabricated on a 40 mm × 20 mm × 3 mm PMMA plate with a CNC device. A quartz capillary was inserted as the main channel for introducing the continuous phase and providing reaction space, while another thinner quartz capillary was coaxially inserted inside the outer capillary as the dispersed phase flow channel. The outer and inner diameters of the main channel were 0.70 mm and 0.53 mm, respectively. The outer and inner diameters of the inserted channel were 0.29 mm and 0.19 mm, respectively. The reaction time for polymerization was adjusted by changing the length of the main capillary or flow velocity. Two gastight syringe needles were inserted from each side of the PMMA substrate as continuous phase inlets. The coaxial capillary device was sealed using another 3 mm PMMA plate with a supersonic-assisted sealing technique.[41] To ensure that no liquids leaked out of the microdevice, an adhesive (3M, USA) was used to fill the gaps between the inserted parts (quartz capillary and syringe needle) and the channels fabricated on the PMMA plates.

Experimental Procedure for the Microreactor. BA monomer with a set AIBN ratio (ranging from 0.2 to 1% per mole of monomer), was used as the dispersed phase. Water containing

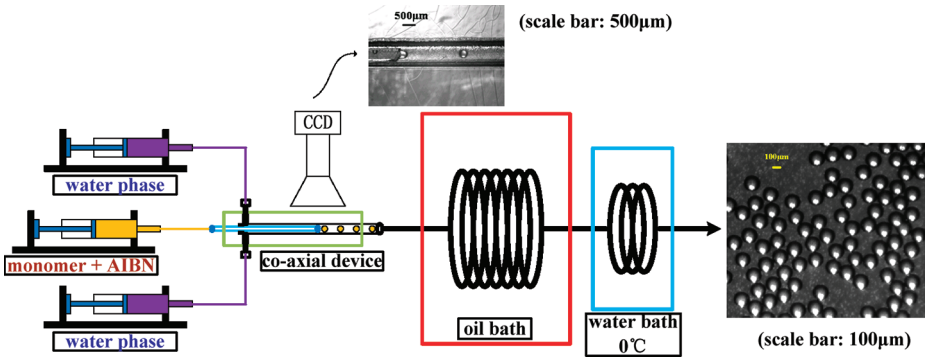

Figure 2. Outline of experimental procedure in microreactor.

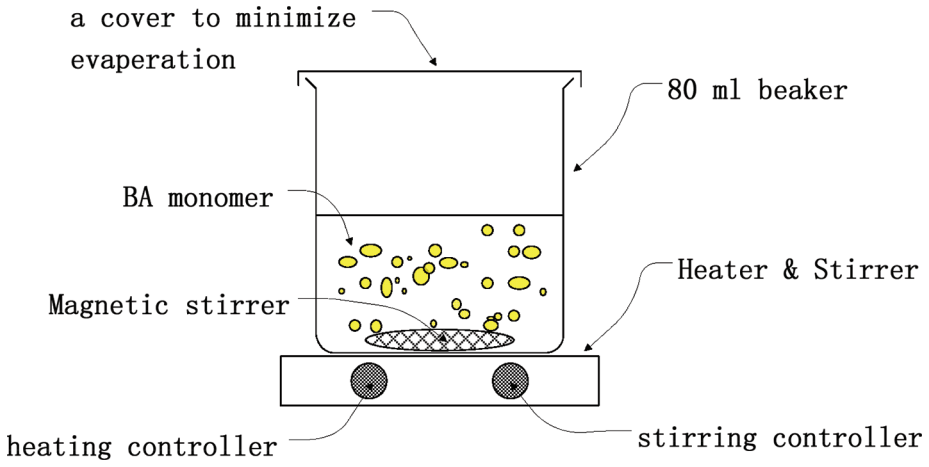

Figure 3. Scheme of setup of batch reactor.

surfactants and a stabilizer (SDS, 0.5 wt %; PVA, 0.5 wt %; Na_2SO_4, 0.3 wt %) was used as the continuous phase.

Figure 2 provides a layout of the experimental procedure. Two microsyringe pumps (TS-1B/W0109-1B, Longer, China) were used to pump the two phases into the microreactor. The BA monomer solution was dispersed into uniform droplets by the sheath focusing force of the water phase flowing from the two side channels. To prevent partial polymerization of BA before dispersion, ice bags were placed on the syringe containing BA monomer and the tube between that syringe and the coaxial micro device. A microscope with 20−200× magnification coupled with a high-speed CCD video camera (PL-A742, PixeLINK, Canada) was used to observe the flow pattern and droplet size in the microreactor.

After steady drop flow in the capillary was achieved, the droplets were then heated in an oil bath to initiate and carry out the polymerization process for a set reaction time. A cold water bath was used to stop polymerization. The product, collected at the end of the capillary, was washed and dried under vacuum to remove monomer and water.

Comparative Experiments in Stirred Container. For comparison purposes, the polymerization was also carried out in an 80 mL glass beaker (inner diameter, 46.1 mm; thickness of wall, 2 mm), as shown in Figure 3. An electrical heater with a magnetic stirrer was used to heat the water phase and disperse the monomer. In experiments, the water phase was introduced first and preheated to 100 °C before the monomer solution was added. The temperature was set to remain constant throughout the reaction. In order to minimize water evaporation, a cover was placed over the top of the beaker. After the required reaction time was reached, polymerization was quenched by cooling the reactor within an ice−water bath.

2.3. Analysis. GPC analysis was carried out on a Waters-515 gel permeation chromatograph equipped with a refractive index detector. The number-average molecular weight (M_n) and the polydispersity index (PDI, referred to as M_w/M_n, where M_w is the weight-average molecular weight) of synthesized polymers were determined at 40 °C in THF using polystyrene standard samples for calibration.

Conversion was measured using the gravimetric method.

3. RESULTS AND DISCUSSION

3.1. Operating Conditions in the Coaxial Capillary Microreactor. In the microreactor, it is crucial that experiments be executed in a uniform droplet flow regime. Therefore, flow patterns in the coaxial microreactor were investigated first. The results are shown in Figure 4. Three regimes were identified: dripping flow, slug flow, and a transitional region, when the flow rates of BA monomer and the continuous water phase were in the ranges 5−50 and 50−800 μL/min, respectively. Stable uniform droplet flow could be formed in a wide range of flow rates when the flow rate of BA monomer was in the range 5−50 μL/min. In the following sections, all the experiments were carried out in this dripping flow regime.

3.2. Comparison of Coaxial Capillary Microreactor and a Stirred Container. Polymerization of BA was carried out in the coaxial capillary microreactor and stirred container under identical experimental conditions. Table 1 shows the experimental results. Comparing the polymer properties (PDI and M_n) obtained in the microreactor with those obtained in the stirred container at approximately the same conversion level, it can be seen that the PDI in the microreactor is much lower and the M_n is much larger. As for the reasons responsible for lower PDI in the microreactor, there are two. First, in the microreactor the polymerization units are highly uniform, and product properties will be the same for each individual droplet. In the micoreactor, the BA droplet was dispersed in the continuous phase in a highly uniform manner, while in the stirred container, the droplet size was widely variable, as seen in Figure 6a. Second, the heat transfer efficiency is high enough to avoid heat accumulation in droplets during polymerization. The latter assumption will be further justified by the CFD simulation shown below.

The reduced average molecular weight in the macroreactor could be explained by an autoacceleration phenomenon. As a highly exothermic and thermally initiated free radial reaction, there exists an autoacceleration phenomenon in the BA polymerization process due to strong coupling between reaction and transport phenomena. Once the heat removal becomes insufficient, reaction temperature increases sharply. As a consequence, this sudden rise in temperature further accelerates the overall rate of polymerization as well as the rate of heat release. In addition, the termination rate is reduced due to a diffusion limitation brought about by an increase in viscosity, and hence a gel effect takes place. Both the above factors lead to faster decomposition of initiator and result in polymers with shorter chains (smaller average molecular weight).

The reproducibility of polymerization in the microreactor was also investigated by repeating experiments under identical conditions. As shown in Figure 5, the experimental results indicate that the reproducibility in conversion, M_n, and PDI of the product is quite good.

In the stirred container, the size of the droplet was widely distributed (Figure 6a), and droplet coalescence posed a serious problem (Figure 6b). Thus, the local reaction conditions of BA polymerization, including temperature, were hardly uniform. In some regions, localized high temperatures may have led to instantaneous polymerization, generating polymers with shorter chain length as well as branched polymers and hence further contributing to a wider molecular weight distribution.

3.3. Temperature Profile in the Coaxial Capillary Microreactor. The local reaction temperature in the droplet for a suspension polymerization method is a critical factor influencing the BA polymerization process. CFD simulation can help calculate the temperature profile and its variance as the polymerization proceeds. Considering the uniform drop flow in a coaxial capillary microreaction, a single droplet model was proposed. In our experiments, the flow velocity in the capillary is rather slow (on the order of 0.01 m/s). Furthermore, because the BA droplet is flowing along with the continuous phase and there is no conspicuous relative velocity along the axis of the tube length, heat transfer only takes place between the droplet and the specific volume of water that encompasses it. Based on these facts, as well as for the purpose of simplifying the simulation, hydrodynamics were not considered in the model. The transient state governing equations, including coupled partial differential equations resulting from heat transfer (conduction) and mass transfer (diffusion and chemical reactions), are

$$\rho C_p \frac{\partial T}{\partial t} + \nabla\cdot(-\kappa\nabla T) = Q \quad (1)$$

$$\frac{\partial C_i}{\partial t} + \nabla\cdot(-D_i\nabla C_i) = R_i \quad (2)$$

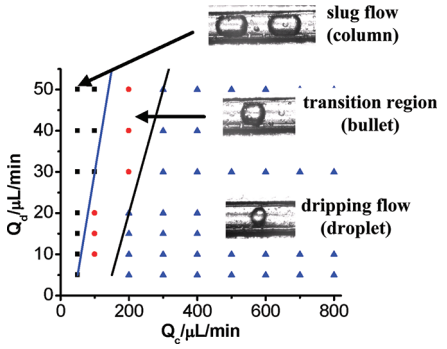

Figure 4. Flow pattern with different flow rates of two phases.

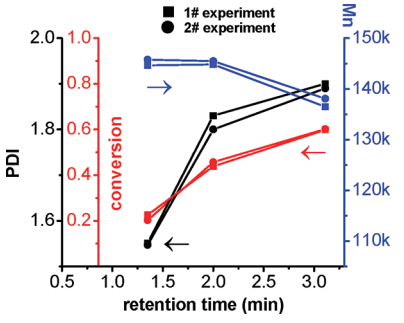

Figure 5. Reproducibility of product's conversion, M_n, and PDI in microreactor. Oil bath temperature, 100 °C; length of the capillary in oil bath, 2 m; AIBN concentration, 0.8%; flow ratio, Q_d(μL/min)/Q_c(μL/min), 15/400, 10/200, and 5/130, from left to right.

Table 1. Comparison of Product Properties in Different Reactors

reactor	AIBN, %	temp, °C	phase ratio	reaction time, min	conv, %	PDI	M_n
microreactor				1.35	50.16	1.55	175 768
	0.8	100[a]	Q_d, 20 μL/m; Q_c, 400 μL/m	2	67.92	1.80	145 477
				3.11	70.16	1.89	138 083
stirring tank				5	50.00	3.11	81 296
	0.8	100	BA, 2 mL; water, 40 mL	10	70.27	3.70	57 132
				15	72.08	7.83	20 291

[a] Oil bath.

dx.doi.org/10.1021/ie201497b |*Ind. Eng. Chem. Res.* 2011, 50, 11853–11862

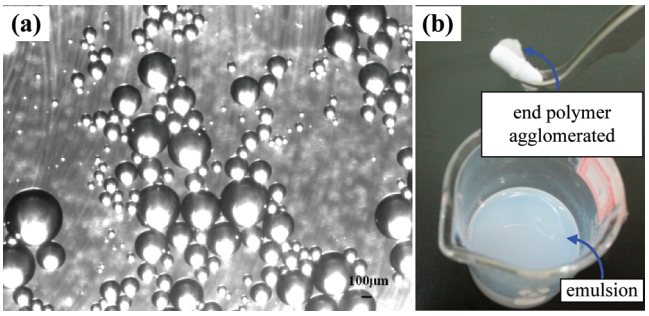

Figure 6. (a) Droplet size distribution in stirring tank. (b) Photograph of poly(butyl acrylate) obtained in the stirring tank, which illustrates that severe agglomeration took place.

The method of moments was introduced for modeling the polymerization kinetics. This method is a straightforward and useful approach to handle polymerization kinetics, and has been successfully applied to yield a truncated set of moment equations as a solution for providing an adequate description of a polymerization process.[42] By using the method of moments, the number of chemical species involved is greatly reduced, and the polymerization kinetics can be easily solved using commercial CFD software. The basic theory and procedure for this method are briefly described below.

For free radical polymerization, the kinetic chemical equations have the following simplified formats:

$$\mathrm{I} \xrightarrow{k_d} 2\mathrm{I}^{\bullet} \qquad \text{initiator decomposition}$$

$$\mathrm{I}^{\bullet} + \mathrm{M} \xrightarrow{k_i} \mathrm{P}_1^{\bullet} \qquad \text{initiation step}$$

$$\mathrm{P}_n^{\bullet} + \mathrm{M} \xrightarrow{k_p} \mathrm{P}_{n+1}^{\bullet} \qquad \text{propagation step}$$

$$\mathrm{P}_n^{\bullet} + \mathrm{P}_m^{\bullet} \xrightarrow{k_t} \mathrm{M}_{m+n} \qquad \text{termination by combination}$$

where I represents the initiator, $\mathrm{I}^{\bullet}$ is the primary radical, M is the monomer, $\mathrm{P}_n^{\bullet}$ is the living polymer of chain length n, M_n is the dead polymer of chain length n, and k_x are the kinetic constants of the specific reactions.

Introducing the zero, first, and second moments of the living and dead polymer distributions:

$$\lambda_i = \sum_{n=1}^{\infty} n^i C_{\mathrm{P}_n\bullet} \qquad i = 0, 1, 2$$

$$\mu_i = \sum_{n=1}^{\infty} n^i C_{\mathrm{M}_n} \qquad i = 0, 1, 2$$

Then, the reaction rate of the different species could be described as

$$R_{\mathrm{I}} = -k_d C_{\mathrm{I}}$$

$$R_{\mathrm{M}} = -k_p \lambda_0 C_{\mathrm{M}}$$

$$R_{\mu_0} = \frac{1}{2} k_t {\lambda_0}^2$$

$$R_{\mu_1} = k_t \lambda_0 \lambda_1$$

$$R_{\mu_2} = k_t (\lambda_0 \lambda_2 + {\lambda_1}^2)$$

Table 2. Data of Physical Properties Used in CFD Simulation[44,45]

	water phase	BA monomer	quartz capillary
molar heat capacity, C_p, kJ/(kg·K)	4.220	1.939	0.739
density, ρ, kg/m^3	998	861	2650
thermal conductivity, κ, W/(m·K)	0.599	0.127	1.482

Table 3. Kinetics Data Used in CFD Simulation

	expression	description	ref
k_d, s^{-1}	$(1.59 \times 10^{15})e^{-15504/T}$	decomposition rate constant of AIBN	46
k_p, m^3·mol^{-1}·s^{-1}	$(2.31 \times 10^{4})e^{-2177/T}$	propagation rate constant of BA	47
k_t, m^3·mol^{-1}·s^{-1}	$(2.57 \times 10^{5})e^{-673/T}$	chain termination rate constant of BA	48

To close the equations above, the quasi steady state approximation (QSSA) was applied and then the moments of the living polymers distribution can be expressed by

$$\lambda_0 = C_{\mathrm{P}\bullet} = \sqrt{\frac{2k_d f C_{\mathrm{I}}}{k_t}}$$

$$\lambda_1 = L\lambda_0$$

$$\lambda_2 = 2\lambda_0 L^2$$

where f is the initiation efficiency and L is the kinetic chain length, which has the following expression:

$$L = \frac{k_p \lambda_0 C_{\mathrm{M}}}{2k_d f C_{\mathrm{I}}}$$

Considering that the propagation step is the main contributor to the heat released by the polymerization, the heat source is given by

$$Q = -\Delta H_p k_p C_{\mathrm{P}\bullet} C_{\mathrm{M}} = -\Delta H_p k_p \lambda_0 C_{\mathrm{M}}$$

where ΔH_p is the enthalpy of the propagation reaction; for butyl acrylate, it is equal to 78 kJ/mol.[43]

The physical properties used in the simulation are shown in Table 2. Kinetics data for AIBN decomposition and polymerization of butyl acrylate are given in Table 3. As reported, the kinetics for free radical polymerization of butyl acrylate are unique in that branching and scission cannot be neglected, mainly due to the fact that secondary propagating macroradicals (SPRs) can easily transfer radical functionality to a different position within the polymer chain, creating a midchain radical (MCR).[49] However, the main objective of the CFD simulation in the present work is to calculate the temperature profile within the BA droplet and provide deeper insight into the superiority of the microreactor in coping with highly exothermic polymerization reactions. Investigation into the polymerization kinetics and prediction of polymer properties such as molecular weight and polydispersity index are not within the scope of this work. Therefore, in order to simplify the mathematical modeling of the kinetics, the MCR

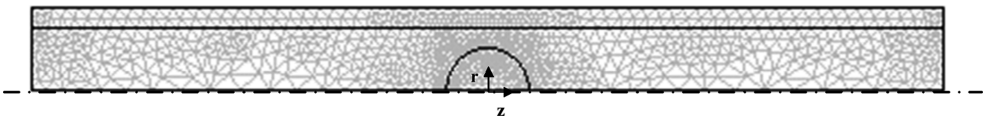

Figure 7. Typical mesh used for simulation.

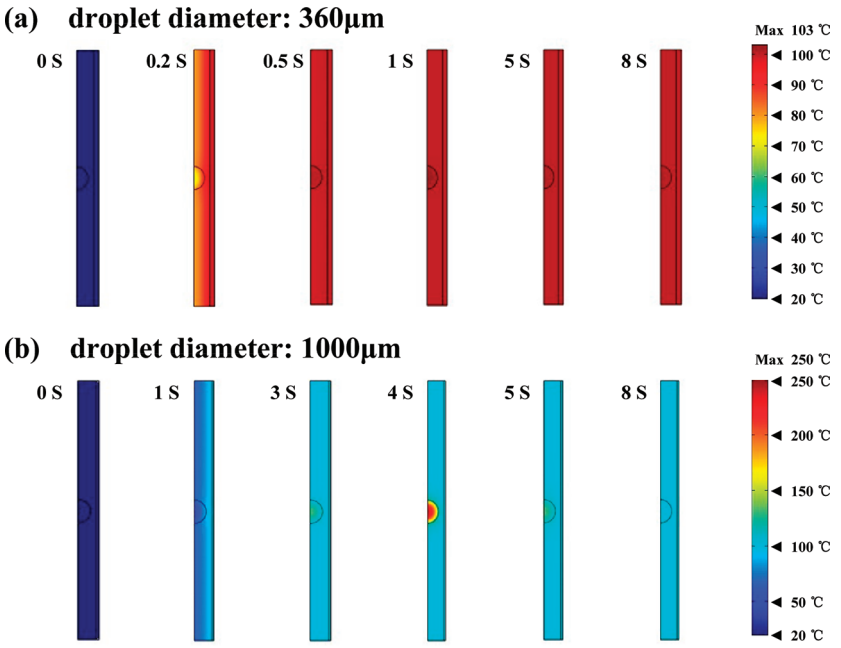

Figure 8. Comparison of temperature profiles simulated by CFD method.

effect on polymerization kinetics as well as the diffusion controlled termination mechanism was not considered in the single droplet model.

Another important parameter in the CFD simulation was the diffusion coefficients of chemical species. As it is hardly possible to determine the accurate diffusion coefficient for a species in the polymerization system (it is particularly difficult for macromolecular species), all diffusion coefficients of the chemical species involved in polymerization were set artificially. The diffusion coefficients for the monomer and the initiator were assumed to be 10^{-8} m^2/s, whereas the diffusion coefficients for dead polymer distributions (μ_0, μ_1, and μ_2), were assumed to be 10^{-11} m^2/s because dead polymers have a much slower diffusion rate than the monomer and the initiator.

By introducing the above-mentioned assumptions, simplified calculations could be made to yield qualitative results about the heat transfer phenomenon in the polymerization process.

COMSOL Multiphysics 3.4, a commercial software, was used to solve eqs 1 and 2 using the finite element method and the direct linear system solver UMFPACK. In order to reduce the memory required to run the simulations, a two-dimensional axial symmetry model was employed. A finer mesh was used at the droplet boundary. The typical mesh used for the simulation is shown in Figure 7. The initial temperature was set at room temperature of 20 °C. The isothermal boundary condition (T = oil bath temperature) was set at the outer wall of the quartz capillary; thermal insulation boundary conditions were set at outer boundaries other than the symmetry axis. As the polymerization reaction takes place only inside the droplet surrounded by inert continuous phase, a mass insulation boundary condition was set at the phase interface between the water solution and BA monomer.

Parts a and b of Figure 8 correspond to simulation results for droplet sizes of 360 and 1000 μm, respectively. Here, we chose 360 μm to represent the average size of BA droplets generated in the coaxial microreactor and 1000 μm to represent the characteristic size of a typical BA droplet in the macroscale reactor. To make a reasonable comparison, both simulation cases were established according to similar geometries and with the same phase ratio (Q_d/Q_c = 1/20).

Figure 8 shows the temperature profiles within the BA droplets for the first few seconds of polymerization. Figure 8a shows that no heat accumulates in the BA droplet during the entire polymerization process, as indicated by the fact that the highest temperature observed in the polymerization process was 103 °C, nearly identical to the environmental temperature. For 500 μm droplets, the largest droplet size that we can produce in our coaxial capillary microreactor, the highest temperature during polymerization was 105 °C (simulation data not shown). This phenomenon can be attributed to better heat transfer performance due to a reduction in heat transfer distance. Free radical polymerization is a highly exothermic process, and the heat removal rate must be faster than or equal to the rate of heat released by polymerization. In the microreactor, the size of the BA droplet is only several hundred micrometers. This small size not only reduces the amount of monomer involved in polymerization but also greatly improves heat removal efficiency, allowing

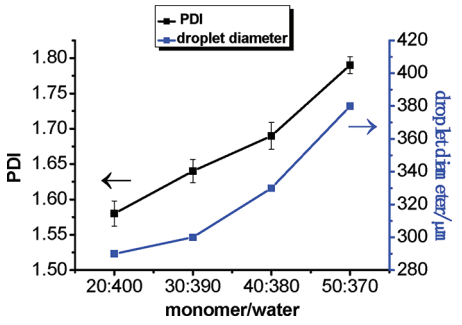

Figure 9. Effect of phase ratio on PDI. Oil bath temperature, 100 °C; length of the capillary in oil bath, 4.5 m; AIBN concentration, 0.8%. The reaction time in the oil bath is about 2.85 min, and the conversions for these samples are 63.36, 60.67, 65.79, and 63.17%, from left to right.

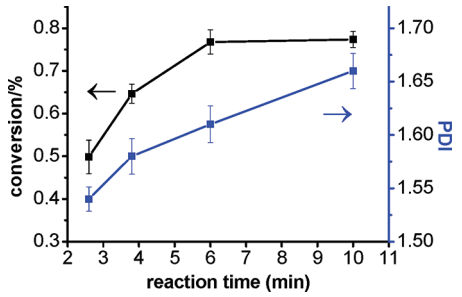

Figure 10. Effect of reaction time on conversion and PDI. Oil bath temperature, 100 °C; AIBN concentration, 0.5%; flow ratio, Q_d (μL/min)/Q_c (μL/min), 10/200.

for the polymerization of BA in a capillary microreactor to be executed in near-isothermal conditions.

Once the size of droplet increases to 1 mm, a different scenario is encountered. Figure 8b shows that a conspicuous hot spot was generated during the polymerization process. The first 3 s comprises a heating stage, where the continuous phase water and BA monomer were heated to the temperature of the heating medium. While at 100 °C, the rates for both AIBN decomposition and chain propagation are very fast, meaning that a large amount of heat was released in relatively short time intervals. At this point, if the heat transfer rate lags behind the rate of heat generation by polymerization, the temperature will increase sharply and in turn will further accelerate the overall rate of polymerization. Explosive polymerization can lead to uncontrolled polymer properties and even potentially hazardous process conditions.

For the 1000 μm sized droplets, the highest temperature observed within the BA droplet was 250 °C. Thus, when the droplet diameter is approximately 1 mm or larger, some monomer in the core of the droplet experiences polymerization under near-adiabatic conditions (adiabatic temperature rise for BA polymerization equals about 250 °C). This indicates that heat transfer is not sufficient in larger droplets, even if the continuous phase encompassing the monomer droplets does remove some heat.

The two simulations discussed above highlight the importance of properly controlling the local reaction temperature when preparing poly(butyl acrylate) with controlled properties. The coaxial microreactor can be used to effectively control the local reaction temperature by reducing droplet size to the submillimeter scale. However, it is rather difficult for commercially used

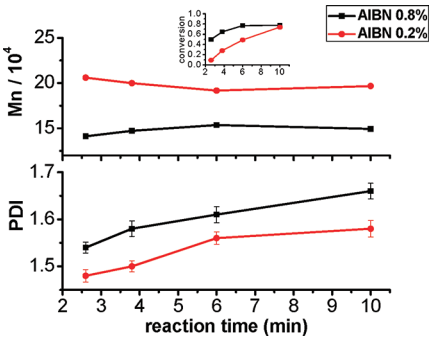

Figure 11. Effect of AIBN concentration on PDI and M_n. Oil bath temperature, 100 °C; flow ratio, Q_d (μL/min)/Q_c (μL/min), 20/400. The inset in the top of the figure represents the corresponding conversions.

macroscale reactors such as stirred tank vessels to achieve the same standard of localized temperature control.

3.4. Factors Influencing Polymer Properties in the Microreactor. *Effect of Phase Ratio.* Figure 9 shows that PDI and droplet diameter increased nearly proportionally with the flow ratio. As discussed in section 3.3, droplet diameter significantly influences heat transfer; therefore it could be speculated that the increase in PDI with flow ratio is due to the increase in droplet size.

Effect of Reaction Time. The effect of reaction time was investigated by adjusting the capillary length. As shown in Figure 10, the PDI increased with reaction time. This trend could be explained by the diffusion controlled termination mechanism. With the reaction time increasing, both the conversion and viscosity within the droplet increase. The rise in viscosity limits the diffusion of macroradicals and slows down the chain termination rate. Therefore, longer reaction times involve larger viscosity disparities and ultimately result in wider molecular weight distributions.

Effect of AIBN Concentration. Higher AIBN concentration means higher radical concentration and faster polymerization. As shown in Figure 11, when the concentration of AIBN increased from 0.2 to 0.8%, the average molecular weight showed a considerable decrease. A faster polymerization rate also generates heat faster, so at higher AIBN concentrations, a larger PDI was observed. Depending on the AIBN concentration, polymers with different average molecular weights could be obtained.

Effect of Reaction Temperature. Figure 12a shows the reaction time vs conversion curves at different oil bath temperatures. Clearly, increasing the reaction temperature could increase the polymerization rate. From Figure 12a , no trend of autoacceleration was detected.

Figure 12b shows a comparison of different PDIs obtained at approximately the same conversion level yet under different reaction temperatures. Higher temperatures involved higher initiation rates and heat generation and resulted in broader molecular weight distributions. These broader molecular weight distributions were also most likely influenced by the enhancement of disordered propagation and termination mechanisms observed at high temperatures, at which the effects of MCR will be more significant.[49]

Figure 12c shows the corresponding average molecular weight. As seen, at a fixed reaction temperature, the average molecular weight of the obtained polymer was approximately the same. In the macroreactor, it is extremely difficult to adjust the average molecular weight by simply changing the reaction temperature, as the exact polymerization temperature is not easy to monitor or

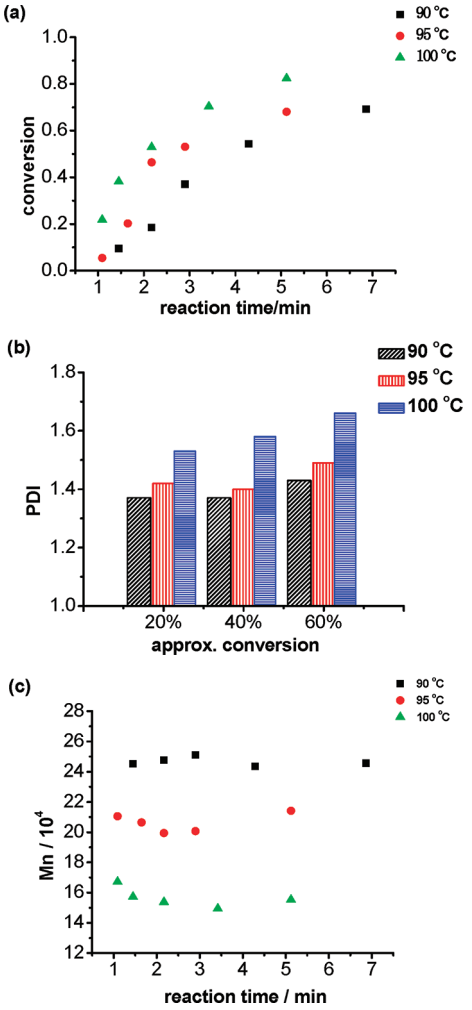

Figure 12. Effect of reaction temperature (referred to as oil bath temperature) on conversion and PDI. AIBN concentration, 0.8%; flow ratio, Q_d (μL/min)/Q_c (μL/min), 5/160.

control. However, in the microreactor, the temperature could be more precisely controlled and the entire polymerization process could be maintained at near-isothermal conditions. Thus, in the microreactor it is possible to adjust the average molecular weight of the final product by changing the reaction temperature.

4. CONCLUSIONS

In this work, a coaxial capillary microreactor was introduced to polymerize butyl acrylate. By reducing the heat transfer distance, the heat generated in the BA polymerization process could be efficiently removed by the continuous water phase, and poly(butyl acrylate) with a narrow molecular weight distribution was successfully prepared. The size of the droplet had a significant influence on heat transfer efficiency, and droplets of smaller diameter were conducive for obtaining narrower molecular weight distributions. A simplified CFD model that could qualitatively calculate the temperature profile within a single BA droplet supported this conclusion. Other factors such as reaction time, oil bath temperature, and AIBN concentration have relatively weak effects on the PDI. The molecular weight of poly(butyl acrylate) could also be adjusted by changing the AIBN concentration and reaction temperature.

A general conclusion from our experimental and numerical results is that the coaxial capillary microreactor exhibits remarkably high efficiency in molecular weight control for highly exothermic free radical polymerization processes due to its superior heat transfer ability. At the same time, using this device, polymers of high molecular weight could be synthesized because the polymerization is realized in monodispersed droplets which do not have direct contact with the channel surface, thereby limiting any unwanted polymer adsorption to the channel wall. This can definitely benefit processes which involve highly adhesive polymers with higher tendencies to adsorb to the reactor surface. Finally, using a coaxial capillary microreactor, polymers were prepared with high reproducibility. Considering all of these advantages, microreactors are also aptly suited for application to studies involving the kinetics of free radical polymerization.

AUTHOR INFORMATION

Corresponding Author

*Tel.: +86 10 62773017. Fax: +86 10 62770304. E-mail: luyc@tsinghua.edu.cn.

ACKNOWLEDGMENT

We gratefully acknowledge the support of the National Natural Science Foundation of China (20525622, 20876084, 21036002, 21176136) and the National Basic Research Program of China (2007CB714302) for this work.

NOMENCLATURE

AIBN = 2,2-azobis(isobutyro)nitrile
BA = butyl acrylate
CFD = computational fluid dynamics
C_i = concentration for ith species
C_p = molar heat capacity at constant pressure
CV = coefficient of variation
D_i = diffusion coefficient for ith species
D_n = dead polymer of chain length n
f = initiation efficiency
GPC = gel permeation chromatography
I = initiator
k_d = decomposition rate constant
k_p = propagation rate constant
k_t = chain termination rate constant
L = kinetic chain length
M = monomer
MCR = midchain radical
M_n = number-average molecular weight
M_w = weight-average molecular weight
PDI = polydispersity index
PMMA = poly(methyl methacrylate)
$P_n^\bullet$ = living polymers of chain length n
PVA = poly(vinyl alcohol)
Q = heat source
Q_c = flow rate of continuous phase
Q_d = flow rate of dispersed phase
R_i = reaction rate for ith species
SDS = sodium dodecyl sulfate
SPR = secondary propagating macroradical
ΔH_p = enthalpy of the propagation reaction
κ = thermal conductivity
λ_i = ith living polymer distribution

μ_i = ith dead polymer distribution
ρ = density

REFERENCES

(1) Meyer, T.; Keurentjes, J. *Handbook of Polymer Reaction Engineering*; Wiley-VCH: New York, 2005.

(2) Achilias, D. S. A Review of Modeling of Diffusion Controlled Polymerization Reactions. *Macromol. Theory Simul.* **2007**, *16*, 319.

(3) Ray, W. H.; Soares, J. B. P.; Hutchinson, R. A. Polymerization Reaction Engineering: Past, Present and Future. *Macromol. Symp.* **2004**, *206*, 1.

(4) Ehrfeld, W.; Hessel, V.; Löwe, H. *Microreactors: New Technology for Modern Chemistry*; Wiley-VCH: New York, 2005.

(5) Hessel, V. Novel Process Windows—Gate to Maximizing Process Intensification via Flow Chemistry. *Chem. Eng. Technol.* **2009**, *32*, 1655.

(6) Yoshida, J.; Nagaki, A.; Yamada, T. Flash Chemistry: Fast Chemical Synthesis by Using Microreactors. *Chem.—Eur. J.* **2008**, *14*, 7450.

(7) Mae, K. Advanced Chemical Processing Using Microspace. *Chem. Eng. Sci.* **2007**, *62*, 4842.

(8) Steinbacher, L. J.; Mcquade, D. T. Polymer Chemistry in Flow: New Polymers, Beads, Capsules, and Fibers. *J. Polym. Sci., Part A: Polym. Chem.* **2006**, *44*, 6505.

(9) Pennemann, H.; Watts, P.; Haswell, S.; Hessel, V.; Löwe, H. Benchmarking of Microreactor Applications. *Org. Process Res. Dev.* **2004**, *8*, 422.

(10) Chen, G. G.; Luo, G. S.; Xu, J. H.; Wang, J. D. Membrane Dispersion Precipitation Method to Prepare Nanoparticles. *Powder Technol.* **2004**, *139*, 180.

(11) Ying, Y.; Chen, G.; Zhao, Y.; Li, S.; Yuan, Q. A High Throughput Methodology for Continuous Preparation of Monodispersed Nanocrystals in Microfluidic Reactors. *Chem. Eng. J.* **2008**, *135*, 209.

(12) Rosenfeld, C.; Serra, C.; Brochon, C.; Hadziioannou, G. High-Temperature Nitroxide-Mediated Radical Polymerization in a Continuous Microtube Reactor: Towards a Better Control of the Polymerization Reaction. *Chem. Eng. Sci.* **2007**, *62*, 5245.

(13) Iwasaki, T.; Nagakib, A.; Yoshida, J. Microsystem Controlled Cationic Polymerization of Vinyl Ethers Initiated by CF_3SO_3H. *Chem. Commun.* **2007**, *12*, 1263.

(14) Nagaki, A.; Tomida, Y.; Miyazaki, A.; Yoshida, J. Microflow System Controlled Anionic Polymerization of Alkyl Methacrylate. *Macromolecules* **2009**, *42*, 4384.

(15) Jeong, W.; Kim, J.; Choo, J.; Lee, E.; Han, C.; Beebe, D.; Seong, G.; Lee, S. Continuous Fabrication of Biocatalyst Immobilized Microparticles Using Photopolymerization and Immiscible Liquids in Microfluidic Systems. *Langmuir* **2005**, *21*, 3738.

(16) Rosenfeld, C.; Serra, C.; Brochon, C.; Hadziioannou, G. Influence of Micromixer Characteristics on Polydispersity Index of Block Copolymers Synthesized in Continuous Flow Microreactors. *Lab Chip* **2008**, *8*, 1682.

(17) Iwasaki, T.; Yoshida, J. Free Radical Polymerization in Microreactors: Significant Improvement in Molecular Weight Distribution Control. *Macromolecules* **2005**, *38*, 1159.

(18) Li., W.; Pham, H.; Nie, Z.; MacDonald, B.; Güenther, A.; Kumacheva, E. Multi-Step Microfluidic Polymerization Reactions Conducted in Droplets: The Internal Trigger Approach. *J. Am. Chem. Soc.* **2008**, *130*, 9935.

(19) Okubo, Y.; Maki, T.; Nakanishi, F.; Hayashi, T.; Mae, K. Precise Control of Polymer Particle Properties Using Droplets in the Microchannel. *Chem. Eng. Sci.* **2010**, *65*, 386.

(20) Lorber, N.; Pavageau, B.; Mignard, E. Droplet-Based Millifluidics as a New Miniaturized Tool to Investigate Polymerization Reactions. *Macromolecules* **2010**, *43*, 5524.

(21) Lorber, N.; Pavageau, B.; Mignard, E. Investigating Acrylic Acid Polymerization by Using a Droplet-Based Millifluidics Approach. *Macromol. Symp.* **2010**, *296*, 203.

(22) Mason, B. P.; Price, K. E.; Steinbacher, J. L.; Bogdan, A. R.; McQuade, D. T. Greener Approaches to Organic Synthesis Using Microreactor Technology. *Chem. Rev.* **2007**, *107*, 2300.

(23) Günther, A.; Jensen, K. F. Multiphase Microfluidics: From Flow Characteristics to Chemical and Materials Synthesis. *Lab Chip* **2006**, *6*, 1487.

(24) Xu, J. H.; Li, S. W.; Tan, J.; Wang, Y. J.; Luo, G. S. Controllable Preparation of Monodispersed O/W and W/O Emulsions in the Same Microfluidic Device. *Langmuir* **2006**, *22*, 7943.

(25) Yang, C. H.; Lin, Y. S.; Huang, K. S.; Huang, Y. C.; Wang, E. C.; Jhong, J. Y.; Kuo, C. Y. Microfluidic Emulsification and Sorting Assisted Preparation of Monodispersed Chitosan Microparticles. *Lab Chip* **2009**, *9*, 145.

(26) Wan, J.; Bick, A.; Sullivan, M.; Stone, H. A. Controllable Microfluidic Production of Microbubbles in Water-In-Oil Emulsions and the Formation of Porous Microparticles. *Adv. Mater.* **2008**, *20*, 3314.

(27) Dendukuri, D.; Tsoi, K.; Hatton, T. A.; Doyle, P. S. Controlled Synthesis of Nonspherical Microparticles Using Microfluidics. *Langmuir* **2005**, *21*, 2113.

(28) Seiffert, S.; Romanowsky, M. B.; Weitz, D. A Janus Microgels Produced from Functional Precursor Polymers. *Langmuir* **2010**, *26*, 14842.

(29) Nie, Z.; Li, W.; Seo, M.; Xu, S.; Kumacheva, E. Janus and Ternary Particles Generated by Microfluidic Synthesis: Design, Synthesis, and Self-Assembly. *J. Am. Chem. Soc.* **2006**, *128*, 9408.

(30) Xu, J. H.; Li, S. W.; Tostado, C.; Lan, W. J.; Luo, G. S. Preparation of Monodispersed Chitosan Microspheres and *in situ* Encapsulation of BSA in a Co-Axial Microfluidic Device. *Biomed. Microdevices* **2009**, *11*, 243.

(31) Lan, W. J.; Li, S. W.; Lu, Y. C.; Xu, J. H.; Luo, G. S. Controllable Preparation of Microscale Tubes with Multiphase Co-Laminar Flow in a Double Co-Axial Microdevice. *Lab Chip* **2009**, *9*, 3282.

(32) Vladisavljević, G. T.; Williams, R. A. Recent Developments in Manufacturing Emulsions and Particulate Products Using Membranes. *Adv. Colloid Interface Sci.* **2005**, *113*, 1.

(33) McClements, D. J. *Food Emulsions: Principles, Practice, and Techniques*, 2nd ed.; CRC Press: Boca Raton, FL, 2006.

(34) Zhao, C. X.; Middelberg, A. P. J. Two-phase Microfluidic Flows. *Chem. Eng. Sci.* **2011**, *66*, 1394.

(35) Xu, J. H.; Li, S. W.; Lan., W. J.; Luo, G. S. Microfluidic Approach for Rapid Interfacial Tension Measurement. *Langmuir* **2008**, *24*, 11287.

(36) Kim, S.; Hwang, H.; Lim, C.; Shim, J.; Yang, S. Packing of Emulsion Droplets: Structural and Functional Motifs for Multi-Cored Microcapsules. *Adv. Funct. Mater.* **2011**, *21*, 1608.

(37) Wang, W.; Xie, R.; Ju, X. J.; Luo, T.; Liu, L.; Weitz, D. A.; Chu, L. Y. Controllable Microfluidic Production of Multicomponent Multiple Emulsions. *Lab Chip* **2011**, *11*, 1587.

(38) Patel, H.; Ein-Mozaffari, F.; Dhib, R. CFD Analysis of Mixing in Thermal Polymerization of Styrene. *Comput. Chem. Eng.* **2010**, *34*, 421.

(39) Maggioris, D.; Goulas, A.; Alexopoulos, A. H.; Chatzi, E. G.; Kiparissides, C. Use of CFD in Prediction of Particle Size Distribution in Suspension Polymer Reactors. *Comput. Chem. Eng.* **1998**, *22*, S315.

(40) Mandal, M.; Serra, C.; Hoarau, Y.; Nigam, K. Numerical Modeling of Polystyrene Synthesis in Coiled Flow Inverter. *Microfluid. Nanofluid.* **2011**, *10*, 415.

(41) Li, S. W.; Xu, J. H.; Wang, Y. J.; Lu, Y. C.; Luo, G. S. Low-Temperature Bonding of Poly-(methylmethacrylate) Microfluidic Devices under an Ultrasonic Field. *J. Micromech. Microeng.* **2009**, *19*, 015035.

(42) McGreavy, C. *Polymer Reactor Engineering*; Blackie Academic & Professional: London, 1993.

(43) Moad, G.; Solomon, D. H. *The Chemistry of Radical Polymerization*, 2nd ed.; Elsevier: Amsterdam, 2006.

(44) Yaws, C. L. *Thermodynamic and Physical Property Data: Comprehensive Thermodynamic and Physical Property Data for Hydrocarbons and Organic Chemicals*; Gulf Publishing Co.: Houston, TX, 1992.

(45) Daubert, T. E.; Danner, R. P. *Data Compilation Tables of Proterties of Pure Compounds*; American Institute of Chemical Engineers: New York, 1985.

(46) Van Hook, J.; Tobolsky, A. The Thermal Decomposition of 2,2′-Azo-bis-isobutyronitrile. *J. Am. Chem. Soc.* **1958**, *80*, 779.

(47) Barner-Kowollik, C.; Günzler, F.; Junkers, T. Pushing the Limit: Pulsed Laser Polymerization of N-Butyl Acrylate at 500 Hz. *Macromolecules* **2008**, *41*, 8971.

(48) Beuermann, S.; Buback, M. Rate Coefficients of Free-Radical Polymerization Deduced from Pulsed Laser Experiments. *Prog. Polym. Sci.* **2002**, *27*, 191.

(49) Junkers, T.; Barner-Kowollik, C. The Role of Mid-Chain Radicals in Acrylate Free Radical Polymerization: Branching and Scission. *J. Polym. Sci., Part A: Polym. Chem.* **2008**, *46*, 7585.